ANKARA YILDIRIM BEYAZIT UNIVERSITY

GRADUATE SCHOOL OF NATURAL AND APPLIED SCIENCES

BLOOD VESSEL SEGMENTATION AND EXTRACTION IN RETINAL IMAGES

M.Sc. Thesis by

Salem.A.Salem.Elhussain

Department of Electrical and Computer Engineering

January, 2018

ANKARA

BLOOD VESSEL SEGMENTATION AND EXTRACTION IN RETINAL IMAGES

A Thesis Submitted to the
Graduate School of Natural and Applied Sciences of
Ankara Yildirim Beyazit University

In Partial Fulfillment of the Requirements for the Master of Science in Electrical and Computer Engineering, Department of Electrical and Computer Engineering

By

Salem.A. Salem.Elhussain

Department of Electrical and Computer Engineering

January, 2018

ANKARA

M.Sc. THESIS EXAMINATION RESULT FORM

BLOOD VESSEL SEGMENTATION AND EXTRACTION IN RETINAL IMAGES

We have read the thesis entitled **"BLOOD VESSEL SEGMENTATION AND EXTRACTION IN RETINAL IMAGES"** completed by **Salem. Elussain** under supervision of **Assist.Prof. Dr. Hilal KAYA** and we certify that in our opinion it is fully adequate, in scope and in quality, as a thesis for the degree of Master of Science. In Department of Electrical and Computer Engineering**.**

Assist.Prof. Dr. Hilal KAYA

(Supervisor)

Prof. Dr. Recep Demirci

(Jury Member)

Assist. Prof. Dr. Baha ŞEN

(**Jury Member)**

Prof. Dr. Fatih V. Çelebi

(Director)

Graduate School of Natural and Applied Sciences

ETHICAL DECLARATION

I have prepared this thesis in accordance with the rules of writing thesis published by the Graduate School of Natural and Applied Science of Ankara Yıldırım Beyazıt University;

- Date I have presented in the thesis, information and documents are obtained in the framework of academic and ethical rules,
- All information, documentation, assessment and results are in accordance with scientific ethics and morals,
- I have given the references for all the works that I used for in this thesis,
- I use the date obtained from the experiments without any change and modification,
- I declare that work presented in this thesis is original,

I understand that all the rights and privileges earned through this thesis can be taken back in the event that any parts of the above decelerations are found to be untrue.

ACKNOWLEDGMENT

All praise to **Allah** today we fold the days' tiredness and the errand collection between the cover of this modest work. To the greatest knowledge lighthouse, to our utmost and most honored prophet **Mohammed** may peace and grace of Allah be upon him.

I would like to express my sincere thanks to my advisor, **Assist. Prof. Dr. Hilal KAYA** for her great support and motivation, her great knowledge and valuable advice constitute a milestone during my studies. Her guidance helped me in my research and writing this thesis.

During my years of study and writing this thesis, I must express my sound gratitude to **my family** for providing endless upholding and constant inducement. Without them, this fulfillment is impossible.

2018, 15 January **Salem. Elhussain**

BLOOD VESSEL SEGMENTATION AND EXTRACTION IN RETINAL IMAGES

ABSTRACT

In this thesis, the retinal vessel segmentation problem is analyzed, and an efficient method is introduced for this approach. The morphological methods are used for the filtering and extraction of the vessels. The advantage of proposed method is low-level complexity and high accuracy rate than the other methods that we compared in this study. For thresholding of the vessel or non-vessel areas, the Otsu method was used. The DRIVE and STARE databases were used for implementation of the method. Sensitivity, specificity, and accuracy metrics are used for evaluation of the proposed algorithm. The average of the accuracy for DRIVE database is 0.9606, and for the STARE database is 0.9598. Finally, for the representation of the proposed method and the all works which implemented in this thesis the graphical user interface (GUI) is used.

Keywords: Image processing, image segmentation, retinal image, morphological methods, Graphical User Interface.

RETİNA GÖRÜNTÜLERİNDE KAN DAMARLARININ BÖLÜTLENMESİ VE ÇIKARILMASI

ÖZ

Bu tez çalışmasında retina damar segmentasyonu incelenmiş ve bu yaklaşım için etkili bir yöntem önerilmiştir. Kan damarlarının filtreleme ve çıkarılması işlemleri için morfolojik yöntemler kullanılmıştır. Önerilen yöntemin avantajı, bu çalışmada karşılaştırdığımız diğer yöntemlere göre karmaşık olmayan işlemler ve yüksek doğruluğa sahip olmasıdır. Kan damarlarının ve damar olmayan alanların eşiklenmesi için Otsu yöntemi kullanılmıştır. Yöntemin uygulanması için DRIVE ve STARE veritabanları kullanılmıştır. Önerilen algoritmanın değerlendirilmesi için duyarlılık, özgüllük ve doğruluk ölçütlerinden faydalanılmıştır. Ortalama doğruluk değeri, DRIVE veritabanı için 0.9606 ve STARE veritabanı için 0.9598 olarak bulunmuştur. Son olarak, önerilen yöntemin bu tezde uygulanan tüm çalışmaların görsel olarak ifade edilmesi için Matlab GUI ortamında bir kullanıcı grafik arayüzü (GUI) geliştirilmiştir.

Anahtar Kelimeler: Görüntü işleme, görüntü bölütleme, retina görüntüsü, Morfolojik yöntem, kullanıcı grafik arayüzü.

CONTENTS

LIST OF ABBRIVIATION

DR	Diabetic retinopathy
DRIVE	Digital retinal image for vessel extraction (retinal image database)
STARE	Structured analysis of the retina (retinal image database)
FOV	Field of view
TP	True positive
TN	True negative
FP	False positive
FN	False negative
Acc	Accuracy
SN	Sensitivity
SP	Specificity
RGB	Red, green and blue color space

LIST OF TABLES

LIST OF FIGURES

CHAPTER 1

INTRODUCTION

1.1 Background

The usage of image processing algorithms to detect vascular procedures in retinal images is becoming increasingly popular. A number of interesting algorithms have already been developed in the field of ophthalmology and in especially intraocular applications. There are few articles about the detection of veins in retinal images. In this thesis, we discuss a few commonly used image processing technique that can be used for vessel segmentation. Also the images which will be segmented and processed are captured from the fundus camera.

In addition to progress in technology, significant developments can be observed in medical applications using the computer analysis techniques. In medical treatment and diagnosis, the methodological analysis for automatic image processing is widely used. Recent developments in the field of medical image processing in particular, enable the automatic detection of various characteristics, changes, diseases and degenerative problems via retinal images. Retinal image analyses use image processing techniques and is aimed at determining and monitoring diseases that can be detected via changes in the structure of the retina.

Fluorescein angiography is considered to be an early method for getting the images of the fundus, or back of the eye, in which the injection of fluorescein is a necessary for blood flow into the bloodstream. However, over the past decade with the developments in information and communication technology, digital fundus photography have been developed on retinal imaging. Fundus imaging is the process of obtaining 3-D projection translucent retinal tissues on a plane imaging the intensity of the reflected light and image representation of the amount of the reflected light. Digital fundus images are widely used in many projects for various reasons. Firstly, available databases that uses patients' fundus photographs were adverted. This type of photography is very useful for the population that were diagnosed with various types

of systemic diseases such as diabetes, vascular stiffness and hypertension. Lastly and the most important advantage of corresponding images is possibility of precise measurement and monitoring of width and tortuosity of retinal blood vessels.

1.2 Retina

The retina is the photosensitive tissue on the domestic surface of the eye (Figure 1.1 (a)). When an ophthalmologist uses an ophthalmoscope to consider the eye, he will see a nerve on retinal image and the entrance point of the main blood supply of the retina. As shown in Figure 1.1 (b), the fovea is in the center of the vessels free reddish spots. The blood vessels of the retina are radiated from the center of the optic disc. The walls of the retinal vessels are transparent, so they can directly observe the blood column that flows in these vessels. Compared with the veins, the arteries look lighter and narrower. The retina is the only part that observes directly the blood circulation system and can detect any changes or abnormalities of blood vessels and can be used for screening. Some pathogens affecting the retina are age-related macular degeneration, glaucoma, retinopathy of prematurity, diabetic retinopathy and hypertension[1]. Some of these diseases can now be automatically identified and evaluated. In addition, the retinal vascular pattern can also provide information about the presence or risk of hypertension, diabetes, cardiovascular or cerebrovascular disease[1].

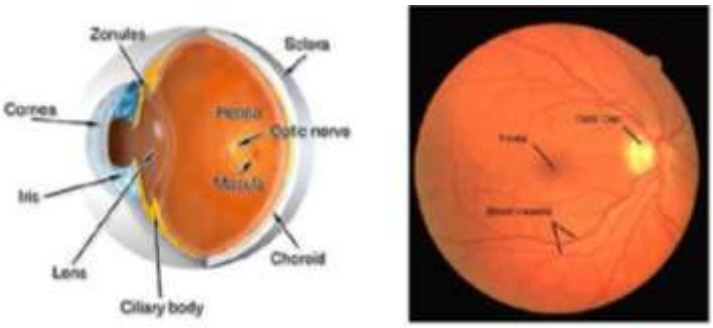

(a) (b)

Figure 1.1 a) Eye anatomy, **b)** Retinal image [2].

The retina is the structure of the eye which is responsible for capturing visual information and transmitting it to the brain. Loss of retinal function leads to irreversible blindness or visual impairment. The retina has a complex perfusion system

with a network of afferent (or arterial) and outgoing blood vessels (arteries or veins). Retinal vein occlusion (RVO) is leading cause of sudden loss of vision in the elderly population (>55 years). Thrombosis (atherosclerosis) is caused by cardiovascular diseases (hypertension, diabetes, high cholesterol). Retinal vein occlusion associated with retinal hemorrhage, vascular leakage and retinal edema and ischemia (hypoxia) can lead to irreversible loss of vision. A completely satisfactory treatment of venous occlusion is not concluded yet. Indication of unloading clotting drugs (TPA, tissue plasminogen activator) can be seen from animal experiments as a possible treatment. However, the very fine retinal blood vessel caliber is an obstacle to drug site. Robot surgery can provide a solution. Figures 1.2 and 1.3 reflect the difference between healthy retina and retina with retinal vein occlusion (RVO).

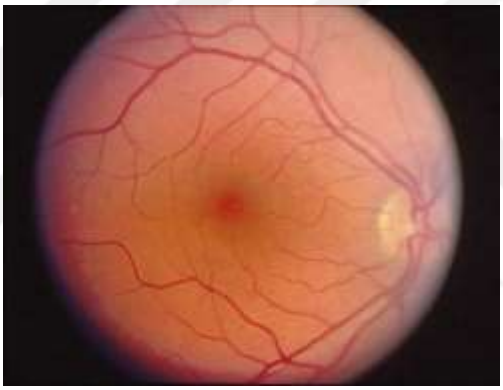

Figure 1.2 Retina right eye: normal [2].

Figure 1.3 Retina right eye: with RVO [2].

1.3 Vessel segmentation

All retinal blood vessels come from the optic disc, and the reflectivity is lower compared to other retinal surfaces, so they are darker than the background. Retinal vascular segmentation is one of the essential components of the automatic retinal disease screening system. Retinal blood vessels and their properties such as length, width, torte, and branch patterns, as well as angles, are useful for the diagnosis, screening, treatment and evaluation of various systemic diseases. Most vascular segmentation uses the contrast between retinal blood vessels and the surrounding background.

1.4 Problem definition and solution

Most retinal images have a high degree of resolution and provide features that can diagnose and treat many diseases when used in clinical areas. The development of automation systems can provide great convenience for hospitals and practitioners. The image processing methods proposed in this study help users to more effectively analyze and diagnose more accurately, regardless of their level of fatigue or image quality, or the individual levels of experience in certain situations and circumstances. In the blood vessel segmentation processes, the segmentation methods sometimes have mistaken pixels for the vessel and non-vessel areas. This is the main important point of this research area. For solving this problem, the morphological operations are proposed. The main advantage of the morphological operations is the low complexity and more accurate results.

1.5 Aim

The aim of our study is to obtain high accuracy of vessel segmentation in the target of retinal images. We will try to take good results in accuracy for segmentation problems. We've had the resultant comparison with other methods. We've also visualized the simulation results on DRIVE and STARE databases. Also, in this thesis, we created the graphical user interface (GUI) for representation of the proposed algorithm to supply an easy application for doctors.

1.6 Motivation

In most cases, the algorithm for retinal vascular segmentation is focused on automatic detection associated with diabetic retinopathy, which is considered to be the leading cause of blindness in recent days. If the disease is found in early stages, treatments can prevent vision loss associated with diabetic retinopathy[3]. Hence, many authors have proposed several different blood vessel segmentation approaches based on different techniques. The complexity and segmentation of the algorithm are different. In this study, different vascular segmentation algorithms are examined and implemented, and their performance is compared with the results provided in the literature.

1.7 Organization of the thesis

Chapter 2 includes a literature review. In this chapter, we discuss the authors' works in retinal vascular segmentation. In Chapter 3, the methodology is described. In Chapter 4, the simulation results are discussed, and the results are compared with other classical methods in the literature. Finally, in Chapter 5, we conclude our thesis with the conclusions and future works.

CHAPTER 2

LITERATURE REVIEW

2.1 Retinal Vessel Segmentation Approaches

One of the most important steps of the retinal image analysis method is the measurement of many important features of blood vessels, depending on the vessel segmentation, the extent of this curvature and the accuracy of vessel segmentation. In this section, a brief review of previously developed methods and algorithms for retinal vein occlusion has been presented. In literature, there are many methods for automatic segmentation of blood vessels in the retina. These methods are divided into two main categories; supervised and unsupervised methods. Rule-named methods for unsupervised methods find vessel locations using prediction rules for vessels. There are five main subcategories based on algorithms; this category itself includes vessel tracking, harmonic filtering, morphological processing, multi-scale analysis and modelling.

2.2 Vessel tracking methods

Methods of tracking vessels use the method of segmenting the map between two points using local information [2, 4-6]. Such approaches are achieved by manually or automatically, following the vessel center lines of the vascular tree by selecting a number of seed spots. There are some important advantages to follow an entire tree without losing time in these areas, providing information about the structure of blood vessels, such as branching and bonding, which does not contain veins, providing very accurate vascular widths, using vessel monitoring methods. The main disadvantage of this method is that it is a method using error to detect the vessels. In addition, these methods are very sensitive to detect vessels with a central reflex.

2.3 Matched filtering techniques

Compatible filtering techniques are based on the two-fold-dimensions core of derivatives with Gaussian or retinal image [7-11]. These methods are carried out by convolving the retinal image with a filter compatible with the recording of the maximum response of each pixel, rotated in various directions of segmentation of blood vessels. Compatible filter core; the diameter and density of vessels have three important attributes that must be considered in design. This method requires a variety of convolution kernels applied to indicate that some rotations capture the different features of the image and the standard deviation parameter of the Gaussian function is that this method is an important task. Moreover, the number of incorrect responses may increase by using different kernels due to the presence of pathologies and retinal background variation which have same features as the vessels in researches that used PSO algorithm for improving the matched filtering [12].

2.4 Morphological techniques

Morphological image processing is a technique based on mathematical operations. Structure elements were applied to the image by morphological operators. The important point that should be noticed is that the image which is processed by the morphological operations must be a binary image. There are several important morphological operations such as dilation, erosion; closing and opening. Dilation expands the objects, erosion shrinks the objects. In this thesis, mathematical morphology procedures were used to improve blood vessels and then used for retinal vessel segmentation. These methods have the advantages of speed and noise resistance.

2.5 Unsupervised method

Another uncontrolled method based on scale-space analysis is the multi-scale approach techniques which use a first and a second derivative of the intensity across the scale field to provide information about the image topology, a multi-based method of measuring retinal blood vessel width, suggested a scale [13]. The multiscale second-order local structure of an image that is called as a Hessian scale, is examined with a

vessel enhancement filter. A measure of the vessel is obtained based on Hessian eigenvalues analysis by using an adaptive filter with fuzzy entropy base [14]. In another study, authors combined the Gauss softening, morphological top-line operator and ship contrast for background development and noise reduction [15].

2.6 Model-based approaches

Model-based approaches include three categories of vessel profile models, active contour models and geometric models [16, 17]. Vessel profile models are selected according to the structure of the vessels. For example, for the vessel cross-sectional intensity profiles, Gaussian shape in the central reflex of the blood vessels is used. There are also other profiles such as second-derivative Gaussian and a replaceable cubic curve. In addition, more complex profiles have gland features such as bright or dark lesions that enhance segment accuracy, and other background features. The active contour models like the snake model is called a curve defined in the image field, which can be able to move under the effect of the internal force of the snake image itself and the force of the external force, which is called a curve defined in the picture field [18]. The lower snake will fit within an image depending on the external and internal definition of the different features. The internal forces give the behavior characteristics of the snake's strain and stiffness and external forces are controlled processes and corrected by the human user. Geometric models are implemented with known special algorithms based on numerical properties as level [19]. These algorithms have interfaces and methods for tracking shapes, i.e. approach of using wavelet transform can be examined in the study of Rodrigues and Marengoni [20].

2.7 Supervised methods

In the supervised methods, the rules of blood vessel extraction are trained by an algorithm based on a training set that is often referred to as a gold standard for manual processing and segmented reference images. The vascular structure of these facts or images are supposed to be gold standards precisely marked by an ophthalmologist. Osareh and Shadgar use multi-scale Gabor filters for vessel candidate identification, and then use principal component analysis to extract features [21]. Xu and Luo proposed a combination of several image processing techniques and vascular

segmentation by using SVM classification [22]. Lupascu et al. introduced another method known as feature-based AdaBoost classifier (FABC) for vascular segmentation [23]. The feature vector encodes a rich description of the characteristics of the vascular-related image, i.e. local (pixel intensity and Hessian-based measurements), the space (for example, the gray profile of the vascular cross section can be approximated by the Gaussian curve) and the structure (for example, the vessel is a geometrical structure, be tubular). You et al. used radial projection and a combination of semi-supervised self-training methods using SVM for vascular segmentation [24]. Improved guided composite wavelet can be used for vascular enhancement. The line strength measures are applied to the vessel enhanced image to generate the feature vector in the previous results. Marin et al. proposed a neural network-based monitoring method for retinal vascular segmentation [25].

2.8 Related works

Before working on proposed methodology, several already imposed methods have been examined. In 2007, Zhang et al. proposed a nonlinear orthogonal projection method for getting the feature from the retinal images and they used the novel local adaptive thresholding method for extraction the vessels. The accuracy average on DRIVE and STARE databases by this methodology is 0.908 and 0.964 [26].

In 2011, Marin et al. proposed a supervised method based on the artificial neural networks. They used momentum and gray level feature extraction methods. The accuracy average on DRIVE and STARE databases obtained by this study is 0.945 and 0.952 [25].

In 2011, Fraz et al. made a division of the power line and multi-scale Gabor and morphological characteristics. The study on the DRIVE and STARE database was tested and obtained an average of 0.947 for DRIVE and, 0.957 accuracy for STARE database [27] .

In 2012, Oliveira et al. proposed a method using match filter combined with filter Frangi and Gabor wavelet filter. Their results were obtained in two ways using the scalable power connectors and Fuzzy C-means (FCM) and they achieve the accuracy of 0.956 and 0.958 respectively [28].

In the year 2013, Asad and others suggested method for vascular division that has three major steps. First step is the usage of image enhancement techniques to enhance the brightness of the retina and then continued through the flooding and extraction of retinal blood vessels. Finally, the structural features of the retinal vascular network were added to the post-treatment phase to improve the phase segmentation results. The proposed method was tested on the database DRIVE and achieved the accuracy degree of 0.937 [29] .

The method proposed by Nguyen et al. in 2013 is based on the length of the baseline detector and the detector lines obtained at different scales. Presentation of the performance of the three datasets on DRIVE, staring and checking the public availability. In the DRIVE and STARE data sets, the proposed method could achieve the accuracy of 0.9407 and 0.9324 [30].

In 2013, Fraz et al. proposed method of segmenting blood vessels of the retina using linear discriminant analysis. The classification utilizes only two linear discriminants for classifying pixels. For the study, DRIVE, STARE and MESSIDOR publicly available data sets were examined. DRIVE database results in accuracy was 0.945, STARE database results in accuracy was 0.951 [31].

In 2014, Emray et al. proposed method, an automated retinal blood vessel segmentation method based on artificial bee colony optimization and fuzzy c - means clustering is presented. DRIVE database results in accuracy was 0.939. STARE database results in accuracy was 0.947 [32].

In 2015, Hassan et al. proposed a method based on mathematical morphology and K-means clustering. The proposed method was tested on datasets in DRIVE database. The experimental results obtained by the proposed method showed that it is useful as accuracy achieved an average of 0.951[33].

In 2015, Hameed et al. proposed a new method of strengthening vessels and pixel tracking algorithm. Pixel tracking algorithm has synthetic background. Stunning performance using the DRIVE and STARE databases and the average accuracy levels achieved were 0.940 to 0.954, respectively [34].

In 2015, Imani et al. proposed a method including the MCA algorithm with appropriate transformation is used to separate blood vessels and lesions from each other. Afterwards, Morlet wavelet transform was used to enhance retinal blood vessels. The final blood vessel graph is obtained by an adaptive thresholding method. For DRIVE and STARE data sets, 0.9523 and 0.9590 accuracy levels were achieved, respectively [35].

In 2015, Mapayi et al. proposed method based on (GLCM) Matrix and entropy were used to study the retinal vascular segmentation. The combination of phase consistency and fuzzy c - mean; value and the combination of phase consistency and gray - level concurrency (GLCM) matrix was used. The proposed method was tested on DRIVE and STARE databases and achieved the accuracy rates of 0.9473 and 0.9354 [36].

In 2016, an effective retinal fundus image segmentation method was proposed. Morphological calculations were used to estimate the vascular structure, and then the Rician Denoise method was used to remove the noise. The proposed method was assessed on DRIVE and STARE databases. The average accuracy of 0.9449 was obtained in the STARE database. The DRIVE database performed an average precision of 0.9435 in segmentation process [37].

In 2017, Fan et al. recommended an unsupervised segmentation algorithm to extract blood vessels from the fundus image. Firstly, they used morphological reconstruction to generate enhanced vascular images, and then divided into three parts: the initial vascular area, the background area. Proposed method was tested on DRIVE, STARE databases, respectively, and achieved 0.960 and 0.957 accuracy precision values in vascular segmentation [38].

CHAPTER 3

METHODOLOGY

This chapter discusses the basic information about the image segmentation and filtering techniques. The Color Space Conversion, Background Subtraction, the detection of veins in the retina, Hybrid Retinal Image Registration, Threshold method, Median Filtering and Morphological Operation on retinal fundus images are investigated in this chapter. This section also introduces the development of a graphical user interface (GUI) for data analysis of this project.

3.1 Detection of veins in retina

3.1.1 Detection of retinal blood vessels based on nonlinear projection

The usage of image processing algorithms in support of robot / computer assisted procedures has an increasing popularity. Also, in the past, a number of interesting algorithms have been developed in eye surgery and in particular for the intra-ocular applications. In this part of the study, some articles are discussed about the detection of retinal veins in images. Second part examines some commonly used image processing techniques that can be used to include real-time tracking of an instrument on camera images. Both elements are necessary for "visual serving" to apply techniques to support retinal vein cannulation.

The intravenous detection technique is more fully explained in the references [39]. Test stage consists of two parts, core network segmentation and following a single wire. Variety of techniques are used to extract the core from the image. This was done by the classification of each pixel according to local properties. For this, filter matching methods as local adaptive threshold, morphological filtering transformation, and wavelet edge methods are used. More classified pixel vessels should be done for diagnosis, surgery and treatments. This is done by manually or automatically determining the starting point of a vein that makes the vein cut and the algorithm that will follow for each vein until the end. The auto-versioning algorithm uses the fuzzy

K-means algorithm to divide the image into pieces with a similar color, and then to search for the next search location. The core piece [40] is carried by a Kalman filter.

The filtering will connect the noise filters in the image and a score classification for one line. Many divergent points are not considered as a vein. It allows blood stains to be removed on these images, so you can see the veins. Figure 3.2 shows the performance of this algorithm on the test images seen in Figure 3.1. In this technique, detection performance can be enhanced on the images by increasing the contrast.

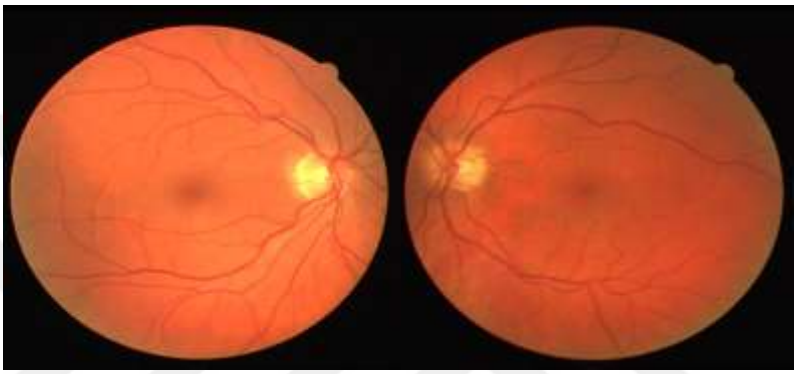

Figure 3.1 Test Image vein [41].

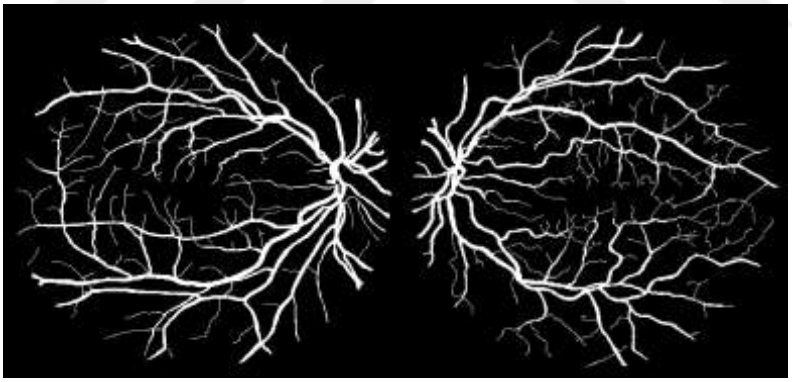

Figure 3.2 Detection of vein.

3.1.2 Hybrid Retinal Image Registration

This vein detection technique is more fully described in [42]. This algorithm is useful for early treatment of diabetic retinopathy. A combination of two techniques can be used that are technical-based, surface-based techniques and features. The technical-based surface primarily uses the density of some optimized object features such as pixels and smallest mean square error, cross-correlation, phase correlation, or feature information. This feature is like a manual recording of a grounded technique. There are similarities between the two pictures and registration will maximize this match.

Firstly, the kernel is determined by taking advantage of a local entropy-based threshold technique. Then based on a binary translation binary image from the first grade, common knowledge is estimated to maximize. Next the image quality is assessed for early treatment of diabetic retinopathy, this is done by the displacement model. Two types of transformations are used with items such as vessels and turning points of sample points. This model provides an affine / quadratic estimate. Three empirical conditions are derived experimentally to check the progress of the algorithm to have as little as possible registry errors and the highest chance of success.

3.1.3 Overview of some general-purpose image processing

The following of a fine needle into the eye gives rise to various problems. Since the needle is exposed from the top, there will be during an operation on the camera images of shade formation action of the needle. Also, there will be reflection arise because the needle has a very glossy surface. For this reason, the needle will be much less visible in the camera images. Also, the designation of the same point of a vein in two different camera images presents a problem. In this section, some image processing techniques are discussed to address these problems.

3.1.4 Color Segmentation

The intention is only to look at the colors that appear in the images. Provided that the needle has a distinctly different color than the rest of the retina would thereby the needle can be quite easily removed from the image. To obtain image must be just to see the needle.

One can use different representations for color segmentation to segment colors: i.e. RGB: Red Yellow Blue. This is a color represented as a combination of the three additive primary colors. To obtain a certain color, a number must be assigned to each primary color and Figure 3.3 shows this model.

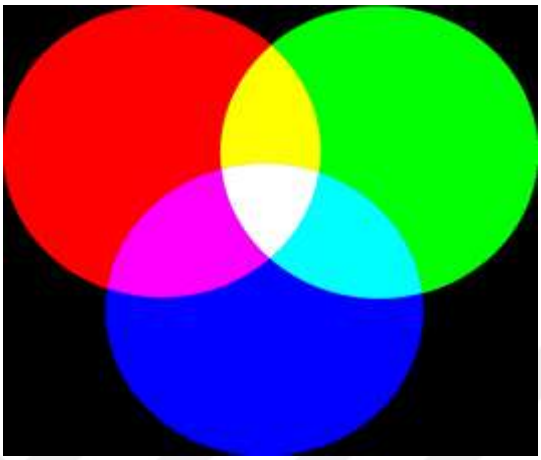

Figure 3.3 RGB [43].

3.1.5 Background Subtraction

Background subtraction is a method that is used to separate the foreground and the background of an image [44]. This is usually used when the camera is firmly mounted. In the simplest case, the camera will always take the same background. Here you can create an image of the background and see what is the difference in the camera afterwards. When there is a change in the image filmed by the camera, this will only be displayed. This is then referred to as the foreground. There are also more complex methods that change the background. The background should be continuously adapted to the environment. Figure 3.4 shows an example of the simple method of background subtraction.

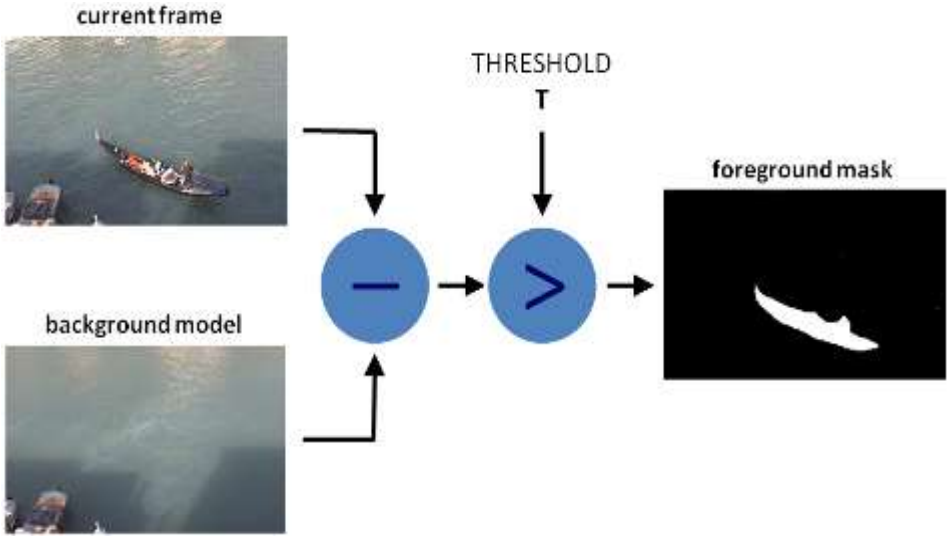

Figure 3.4 Background subtraction [45].

Examining the various image processing techniques discussed in the previous chapter, helped in forming an idea about the beneficial effects of the image processing system.

3.2 Threshold method

The threshold methods include a set of algorithms for segmenting digital images. Segmentation is an important step for image analysis to recognize objects in the image. With the aid of threshold value methods, one can decide in simple situations which picture points represent sought objects and which their surroundings belong to. Threshold methods lead to binary images. The motivation for using the binary images is usually the availability of fast binary image algorithms, for example for blob analysis. Also the storage space savings plays a smaller role in image processing applications today [46].

As with all segmentation methods, pixels are also assigned to the threshold value methods - the so-called pixels - different groups - the so-called segments. The image to be segmented is in the form of numerical values (one or more color values per pixel). The membership of a pixel to a segment is decided by comparing the gray value or another one-dimensional feature with a threshold value. The gray value of a pixel is its pure brightness value; other color information is not considered. Since this operation is usually applied independently for each pixel, the thresholding method is a so-called pixel-oriented segmentation method. Threshold methods are among the oldest methods in digital image processing.

Otsu's well-known method, described in the same section, was published in 1979 by Nobuyuki Otsu. Threshold procedures can be quickly implemented because of their simplicity and segmentation results that can be calculated with little effort [46]. The Otsu method automatically calculates the threshold T based on the input image. This method uses a methodology of performing discriminated analysis by identifying variables that could be distinguished between two or more groups that were naturally generated. The Otsu threshold method involved iterating all possible thresholds and calculating the expansion metrics on either side of the threshold.

A 6-level greyscale image and its histogram are shown in Figure 3.5.

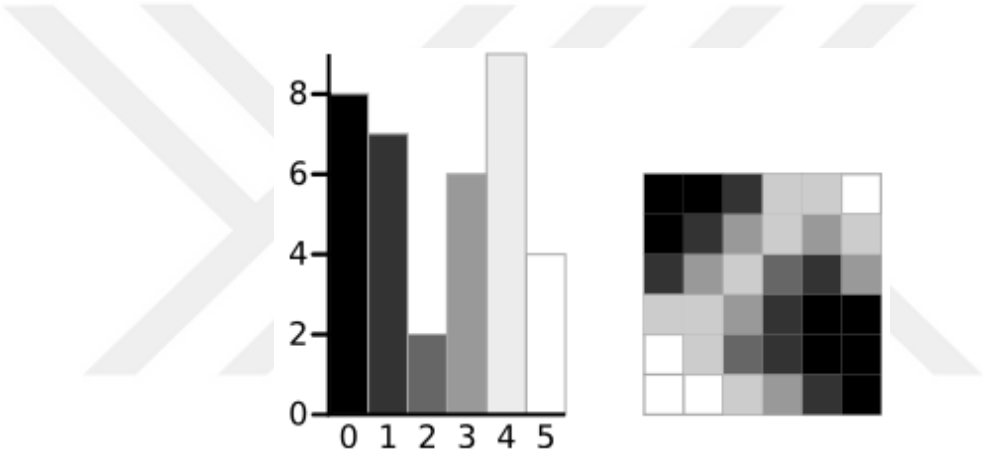

Figure 3.5 A 6-level greyscale image and its histogram [46].

3.3 Graphical User Interface (GUI)

A graphical user interface (GUI) is a form of the user interface of a computer. It has the task of rendering application software on a computer by using graphical symbols, control elements or even widgets. In the case of smartphones, tablets and kiosk systems, this is usually done by using a mouse as a control device with which the graphical elements are operated or selected, usually by touching a sensor screen. The overall design of today's graphical surfaces often uses the so-called desk metaphor. A graphical user interface is based on a window system operating in the graphics mode of the hardware and contains almost always a software component, which makes the control of a computer by pointing devices a dominant control element. An example of the GUI with MATLAB is shown in Figure 3.6.

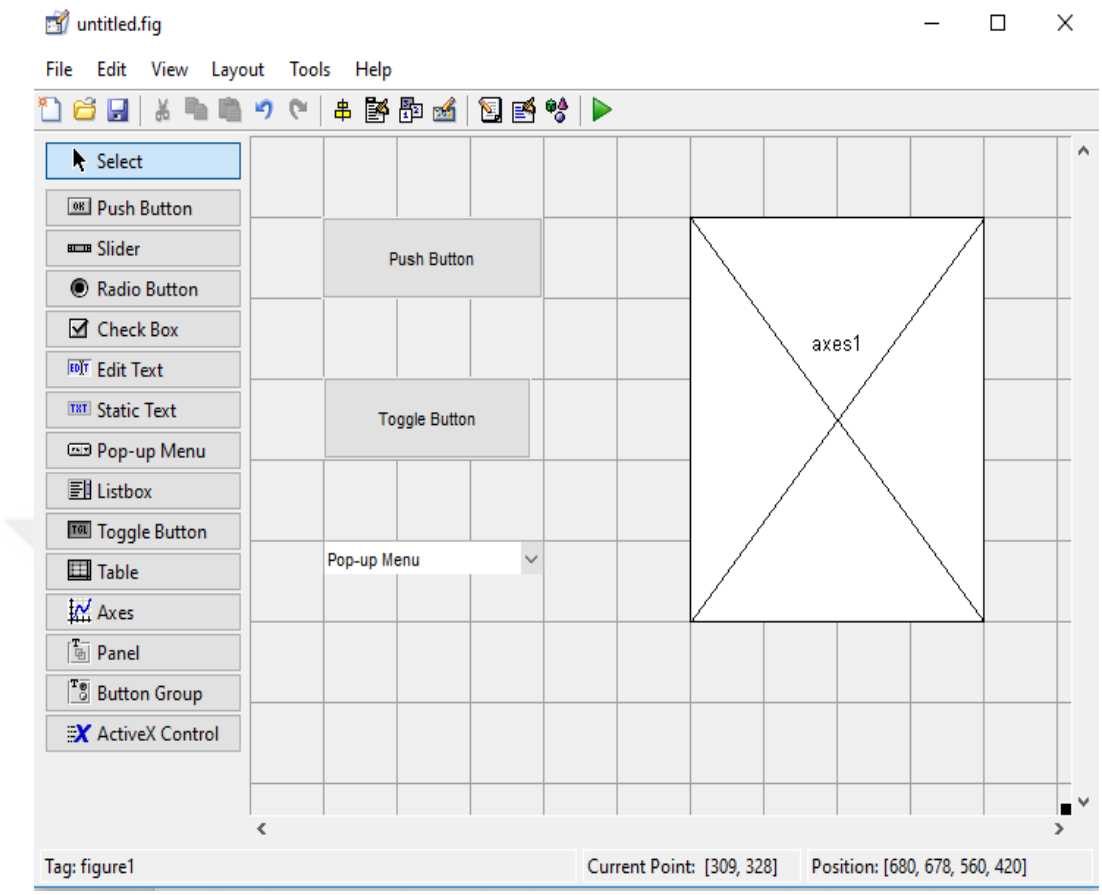

Figure 3.6 An example of the GUI with MATLAB.

3.4 Mathematical morphology

Mathematical morphology is applied more to digital images, but can also be used in graphs, polygonal meshes, solids, and many other spatial structures. Mathematical morphology is also the basis for the processing of morphological images, which consists of a set of operators that transform the images according to the previous characterizations [47].

The generalization after complete reticles is widely accepted today as the theoretical basis of mathematical morphology.

3.4.1 Binary morphology

In binary morphology, an image is viewed a subset of Euclidean space or the entire network for some dimensions.

3.4.2 Structuring element

The main idea is to test binary morphology form of an image with a simple predefined drawing conclusion about how this shape fits or not the shapes in the picture.

3.4.3 Basic Operators

Fixed base operations as shift operators (fixed translated) close to the sum of Minkowski is concerned.

3.4.4 Erosion

The erosion of the binary image A by the structuring element B is defined by:

$$A\Theta B = \left\{ z \in E \middle| B_z \subseteq A \right\} \tag{3.1}$$

Where B_z is the translation of B by the vector z, that is,

$$B_z = \left\{ b + z \middle| b \in B \right\}, \quad \forall z \in E \tag{3.2}$$

In this equation, B is the center.

The erosion of A through B is also given by the expression:

$$A\Theta B = \bigcap_{b \in B} A_{-b} \tag{3.3}$$

3.4.5 Dilation

The dilation of A by the structuring element B is defined by:

$$A \oplus B = \bigcup_{b \in B} A_b \tag{3.4}$$

The dilation is commutative, also given by:

$$A \oplus B = B \oplus A = \bigcup_{a \in A} B_a \tag{3.5}$$

The dilatation can also be obtained by:

$$A \oplus B = \left\{ z \in E \middle| (B^s)_z \cap A \neq \Phi \right\} \quad \textbf{(3.6)}$$

Where B^s denotes the symmetry of B, which is,

$$B^s = \left\{ x \in E \middle| -x \in B \right\} \quad \textbf{(3.7)}$$

As an application example, dilation is the adverse of erosion and the figures that are drawn very faintly thicken when they are "dilated". The easiest way to describe it is to imagine that the same fax/text is written with a thicker pen [47].

3.4.6 Opening

If the image is A and this image take the opening by B that time the operation will done by:

$$A \circ B = (A \Theta B) \oplus B \quad \textbf{(3.8)}$$

The opening is also given by

$$A \circ B = \bigcup_{B_z \subseteq A} B_x \quad \textbf{(3.9)}$$

Which means that it is the locus of the translations of the structuring element B within the image A. In the case of the side square 10 and a radius disc two as a structuring element, the aperture is a side square 10 with the rounded corners, where the radius of the corners is two.

As an application example, suppose someone has written a note on a paper that is not absorbent, so it looks like they are growing small hairy roots all over writing. The opening essentially eliminates the small spilled exterior "lines" and restores the text. The side effect is that it rounds things out and sharp edges begin to disappear.

3.4.7 Close

If the image is A and this image takes the closing by B, that time the operation will done by:

$$A \bullet B = (A \oplus B) \Theta B \tag{3.10}$$

The closure can also be obtained by

$$A \bullet B = (A^c \circ B^s)^c \tag{3.11}$$

The above means that the closure is the complement of the locus of the translations of the symmetry of the structuring element outside the image A [47].

3.4.8 Top-Hat Filtering

Top-hat transform is a grayscale morphological filter that transforms the input grayscale image into another grayscale output image where pixels with a large gray value are the potential crack or crack-like elements. The top-hat transform is defined as following equation:

$$T_w(f) = f \circ b - f \tag{3.12}$$

Here the $T_w(f)$ if transformation of top-hat. The f is figure and o is the opening operation where b is the structural element.

3.4.9 Bottom-hat filtering

The bottom -hat filter enhances the black spots on a white background. It detracts the shape of the image from the original image. After the closure of the expansion, and then erosion. The effect is to fill the hole and add nearby objects. In mathematical morphology and digital image processing, bottom hat transformation is helpful in highlighting the black spots in a given image.

The black top hat transforms. Sometimes referred to as the bottom hat transformation, is given by:

$$T_b(f) = f \bullet b - f \tag{3.13}$$

Where • is the closing operation.

3.5 Mean filter

Average sliding window spatial filter is easy to replace the filter in the center of the window with the average (mean) of all the pixel values in the window. Windows, or kernel, usually square, but can be any shape [47].

unfiltered values

5	3	6
2	1	9
8	4	7

5+3+6+2+1+9+8+4+7=45

45 / 9 = 5

mean filtered

*	*	*
*	5	*
*	*	*

Center value (previously 1) is replaced by the mean of all nine values (5).

3.6 Median Filter

Rank filters belong to non-class linear filters in digital image processing. It has filters that cannot be described by a convolution.

The rank order filters are sorted by the size of the gray values of the pixels collected in a specific environment, the size, and the alignment order. A gray value is selected from this sorted list that takes the place of the gray value of the current pixel. Position selection determines sequential filter pattern.

The minimum filter, pixel gray values, a pixel is collected in a specific environment and sorted by size. Now this sorting list is chosen instead of the gray value of the current pixel, which is the small gray value [47].

For instance, if we consider the nine pixels, one of an odd value (here 222):

5	7	6
7	222	10
6	10	11

The median filter will take the value of the neighborhood by adding the value:

5	7	7	6	**6**	8	8	9	222

And take the median, where the value of 6. Therefore, the output of the filter will give:

5	7	6
7	**6**	10
6	10	11

This makes it possible to replace the outliers by the "consensus" value between adjacent values.

In this thesis, we use the median filter to create the background. The filter provides us a good resolution for container less parts.

The median filter which is widely used in digital image processing because under certain conditions it preserves the edges while eliminating noise. The median filter holds the edge information of the image [47].

3.7 The Databases

The DRIVE and STARE database are used for implementation of the method.

3.7.1 The DRIVE database

Database of DRIVE (Digital Retina Image for Vascular Extraction) collected by Niemeijer et al. (2004) [48] and the images were collected from a DR (Diabetic Retinopathy) screening program. 20 retinal images taken from the DRIVE retina database were used, and 20 retinal images were used for the test. DRIVE retina database was derived from a DR imaging program in the Netherlands. The imaging program included 400 diabetic patients aged 25-90 years, with 40 images randomly selected. Each image was in JPEG format and was shot using a Canon 3CCD camera with a 45-degree image area (FOV). The resolution of the first image is 768 x 584, and each image region is cropped to obtain an image having a resolution of 565 x 584, including a circle having a diameter of about 540 pixels. Figure 3.7 shows retinal images from the DRIVE database [41].

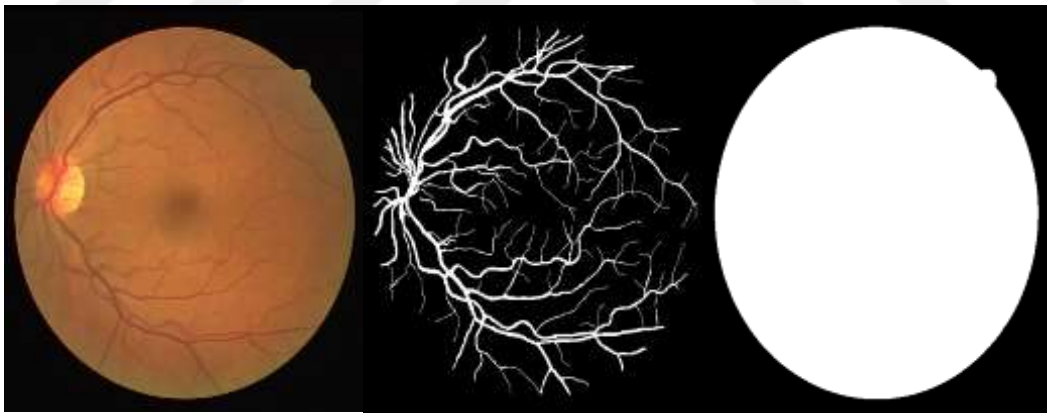

(a) (b) (c)

Figure 3.7 Retinal fundus image 2 from test set of the **STARE** database, **a)** Original **RGB** image [2], **b)** Manual segmentation of blood vessels known as a ground truth, **c)** the **FOV** mask of the corresponding image.

3.7.2 The STARE Database

The database (structure analysis of a retina) STARE [7] contains 20 blood vessel segmentation images, of which 10 are pathological images. Retinal images from the STARE database in Figure 3.8. In a field of view, the Canon BLR-50 fundus camera (FOV) was pulled at 35 degrees. The resolution for photos taken is cropped to obtain images at 500 650 × resolution including 700 605 × and a circle with a diameter of each image area. All photos were manually separated by two auditors. The first advisor is 10.4% segmented pixel and the second advisor is 14.9% segmented vein. As the vein is thin, so the second director of the division than the first director of the most. The performance tag as a reference is calculated by the segmentation of the first observer.

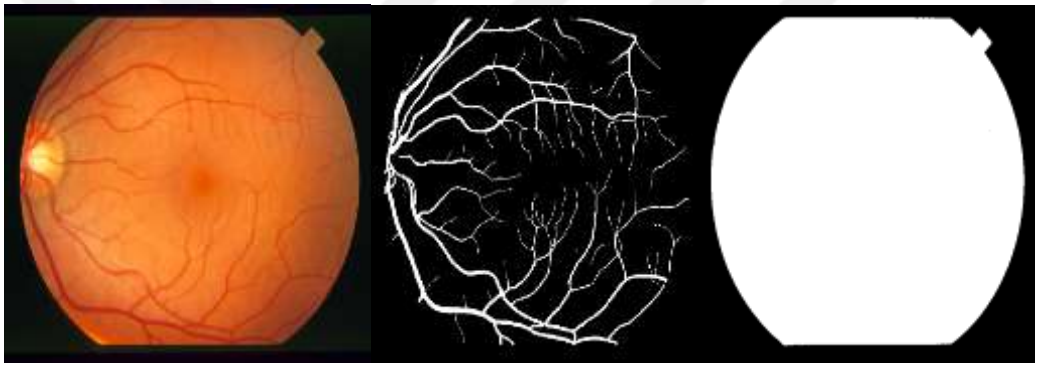

(a) (b) (c)

Figure 3.8 Retinal fundus image 2 from the STARE database of the test set, **a)** Original **RGB** image [2], **b)** Manual segmentation of blood vessels is called ground truth, **c)** The corresponding image of the FOV mask.

3.8 Performance Measures

The calculated performance metrics are sensitivity, specificity, and accuracy using formulas shown in Table 3.1.

Table 3.1 Retinal blood vessel performance segmentation measurement.

Measure	Description
Specificity (SP)	TN / (TN + FP)
Sensitivity (SN)	TP / (TP + FN)
Accuracy (Acc)	(TP + TN) / FOV number of pixels

Where Vessel detected: True positive(TP), False positive(FP).
Vessel not detected: False Negative (FN), True Negative (TN).

I. True positive (TP), if the sample value is positive and the sorting result is positive.
Ii. False Negative (FN), If the sample value is positive and the sorting result is negative.
Iii. False Positive (FP), If the sample value is negative and the sorting result is positive.
Iv. if the sample value is negative and the sorting result is negative, True Negative (TN).

$$Sensitivity = \frac{TP}{TP + FN} \quad \textbf{(3.14)}$$

$$Specificity = \frac{TN}{TN + FP} \quad \textbf{(3.15)}$$

$$Accuracy = \frac{TP + TN}{TP + FN + TN + FP} \quad \textbf{(3.16)}$$

Sensitivity (SN) metrics are the ratio of well-classified vessel pixels. Specificity (SP) metrics are the ratio of well-classified non-vessel pixels. Accuracy is measured as the ratio (FOV) of the pixels that are correctly classified by the total number of pixels in the field of view.

3.9 Summary of Proposed Method

The summary of proposed method is shown in Figure 3.9.

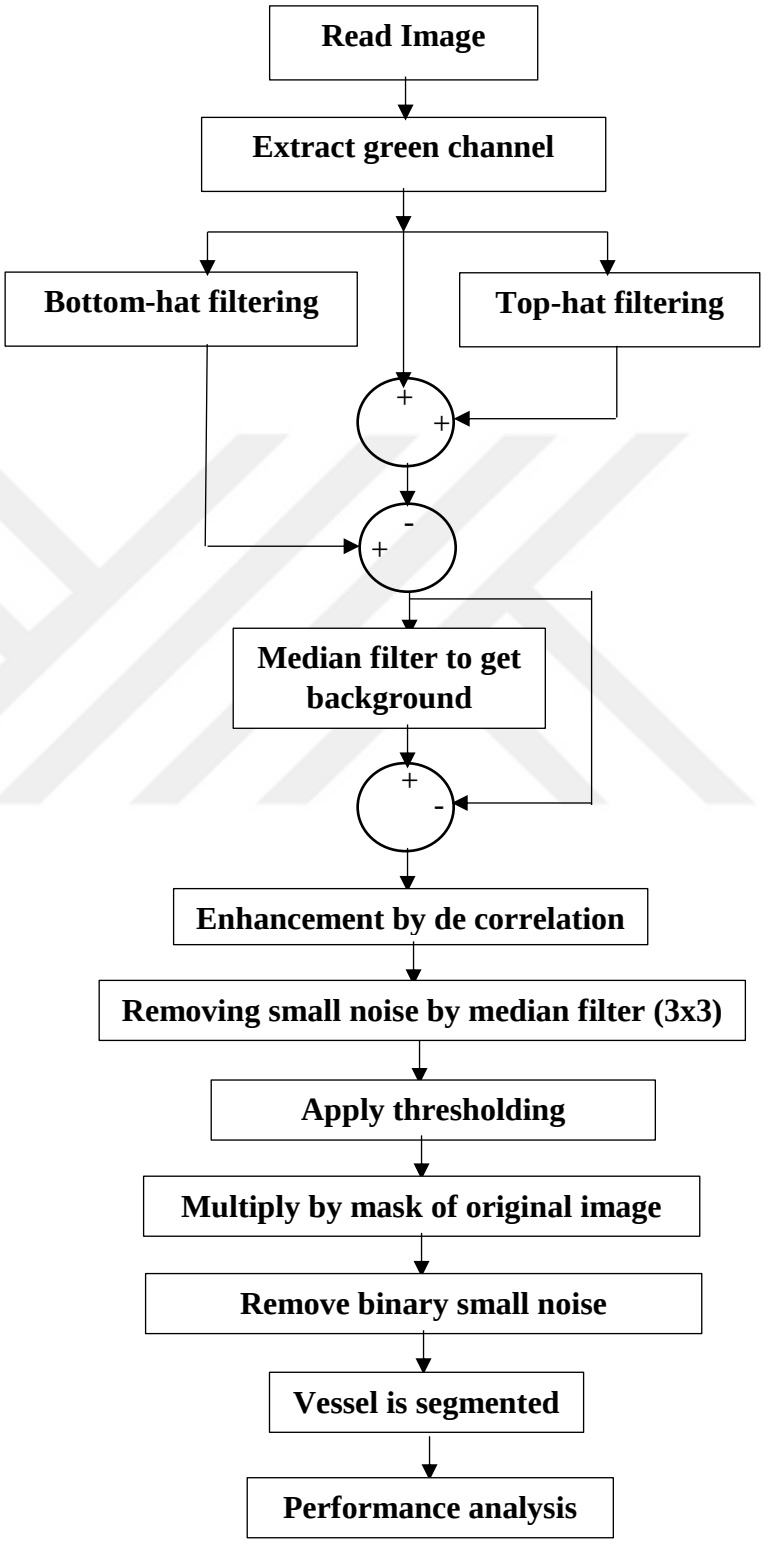

Figure 3.9 The summary for a new process.

CHAPTER 4

SIMULATION RESULTS AND DISCUSSIONS

4.1 Proposed Method

In this thesis, the implementation of proposed method with MATLAB 2016a version is presented. The image processing toolbox and MATLAB fundamental toolbox is used for implementation. For hardware, one personal computer, with Core-i5 the RAM 4GHZ RAM and CPU 2 GHZ is used.

For simulation, the RGB input of the retina image in grayscale images are converted. We convert these images to red channels, green channels, and blue channels. The green channel of the color retinal fundus image has been selected. For segmentation, a green channel image is used, because it increases the contrast between the background plane and the retinal blood vessels. The red and the blue channels are extracted where, it got a bright retinal image in the red channel and too dark retinal images in the blue channel. Differences in channels are shown in Figure 4.1. and Figure 4.2, respectively.

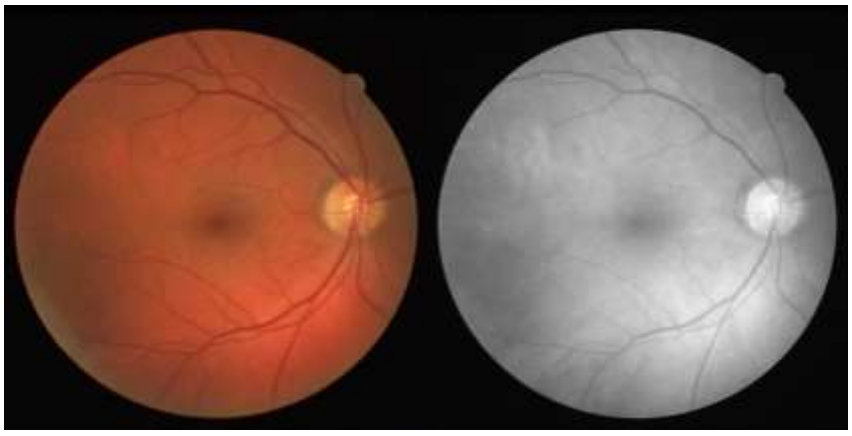

(a) (b)

Figure 4.1 a) Original retina image [41], **b)** Red channel.

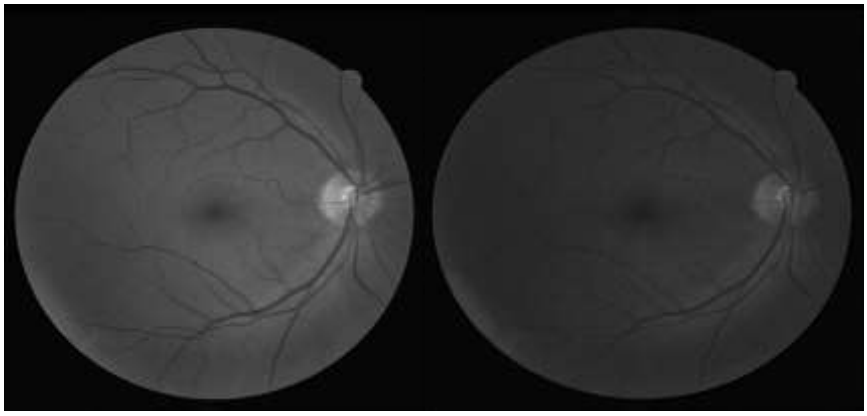

(a) (b)

Figure 4.2 a) Green channel, **b)** Blue channel.

As shown in Figure 4.1. and Figure 4.2, the green channel has more variation between the blood and the background.

In the first step, it is essential to use some classical methods to enhance the original image. In general, the contrast of the retina image is low, and the contrast is required to be improved. For contrast enhancement, morphological element method is used. From green channel image, Bottom-hat filtering and Top-hat filtering are taken. The bottom-hat filters are equivalent to subtract the result of performing the morphological closing operation on the input image from the input image itself. The bottom-hat transformed is used to enhance the dark objects on a light background.

The green channel image and Top-hat filtering result are added, and the result is subtracted with the result of the Bottom-hat filtering. Top-hat transform is used to enhance light objects on a dark background Figure 4.3 illustrates the result.

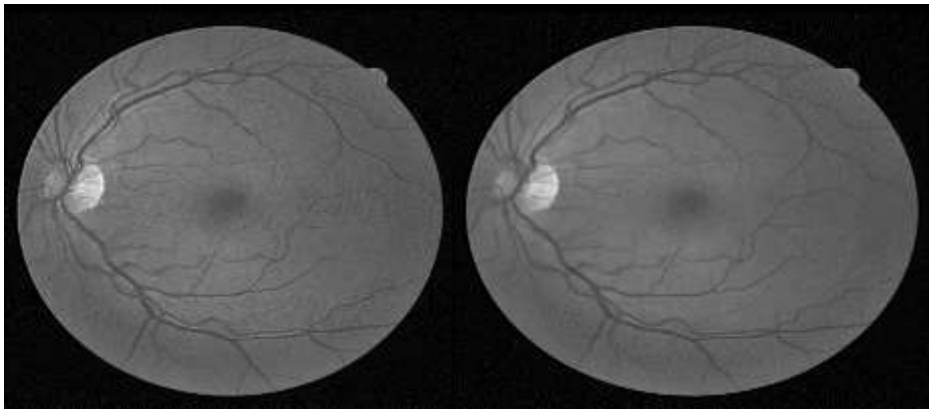

(a) (b)

Figure 4.3 a) Subtract result with Bottom-hat filtering**, b)** original image.

The result shows that the contrast of the image has been improved and the blood vessels are shown clearly.

For getting the background, the median filter is implemented. Actually it needs the blurred image and the median filter with 25*25 which give the best result about background [48]. The median filter result is shown in Figure 4.4.

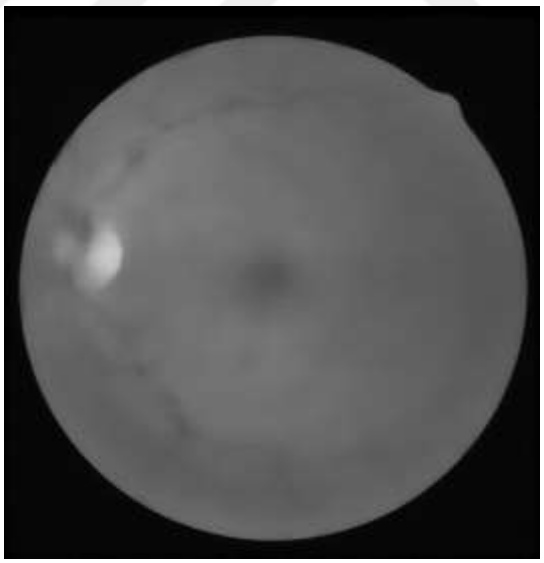

Figure 4.4 Median filter result.

Then the result of the last process is subtracted with the median filter result. Figure 4.5 show this result.

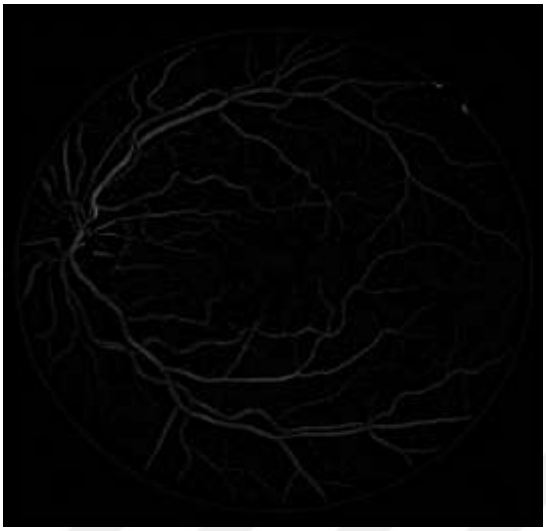

Figure 4.5 Subtracted image with median filter.

The result that is achieved is not so good, and for enhancement of the result de-correlation method is used. This enhancement result is illustrated in Figure 4.6.

Figure 4.6 Enhancement result.

After applying the decorrelation method here had some spot noise, and the median filter with 3x3 window size is used, because of the performance analysis on gray image give high performance for denoising. Spot noise removal result is shown in Figure 4.7.

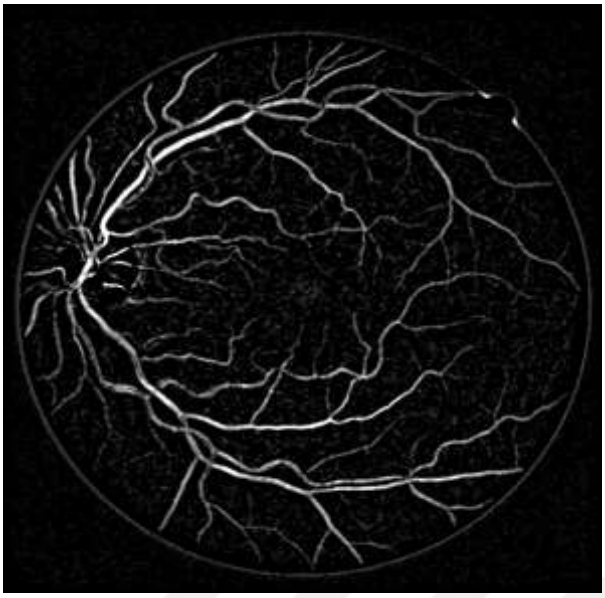

Figure 4.7 Spot noise removal result with median filter.

In next step, the thresholding method for finding the vessel from the image is used. The result of the thresholding is shown in Figure 4.8.

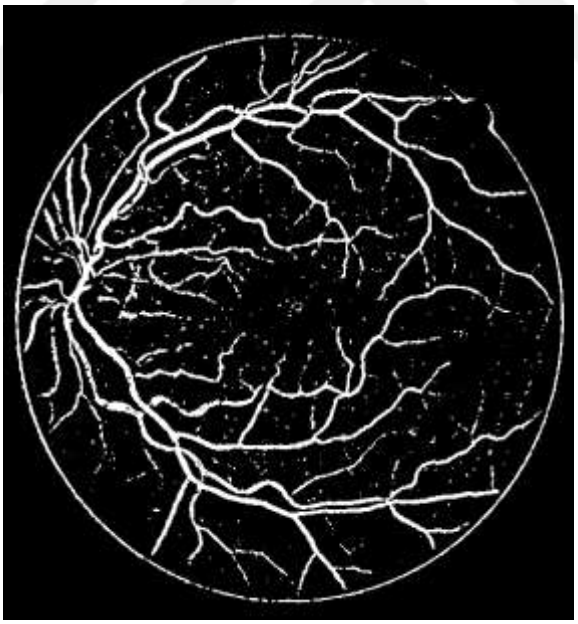

Figure 4.8 Thresholding result.

Finally, multiplied the result with the mask, and the vessel is extracted. The final result of the blood vessel segmentation is shown in Figure 4.9.

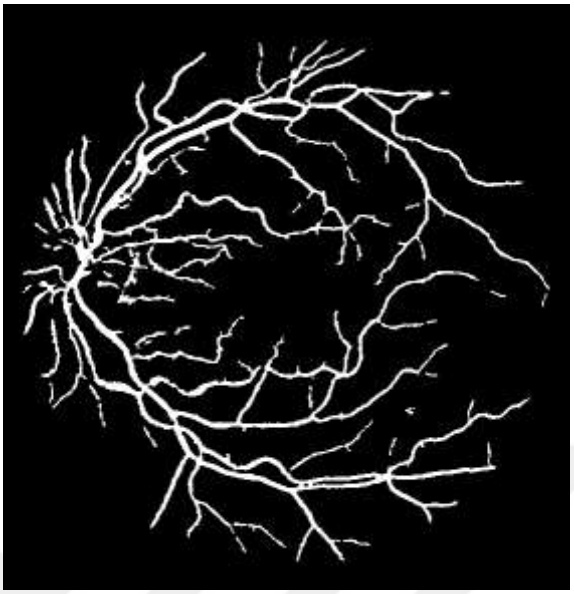

Figure 4.9 Final result of the blood vessel.

4.2 Simulation Results for DRIVE Database

For DRIVE database, the results are in Table 4.1.

Table 4.1 The accuracy results.

Image Number	Sensitivity	Specificity	Accuracy
1	0.76661	0.983199	0.963874
2	0.709411	0.990887	0.962062
3	0.680449	0.982425	**0.952321**
4	0.622554	0.99488	0.960629
5	0.653856	0.989905	0.958422
6	0.654596	0.985603	0.953385

7	0.609147	0.992465	0.957437
8	0.613794	0.989306	0.956998
9	0.650424	0.989024	0.961583
10	0.684232	0.987328	0.962383
11	0.616135	0.992284	0.95861
12	0.706809	0.982167	0.958392
13	0.64568	0.988801	0.955255
14	0.730854	0.982056	0.961747
15	0.702592	0.986342	0.966035
16	0.679534	0.989662	0.961662
17	0.704797	0.985058	0.961401
18	0.727853	0.984468	0.964135
19	0.821892	0.98458	**0.971084**
20	0.779312	0.979054	0.964365
Average	0.6880	0.9870	**0.961**

As shown in the Table 4.1, calculating the average of all images, the accuracy of the fitting method is 0.961. In addition, the highest precision value is 0.971084, the value of image 19 is. The minimum value of image number 3 is 0.952321.

The sensitivity of each image from DRIVE database shows below in Figure 4.10.

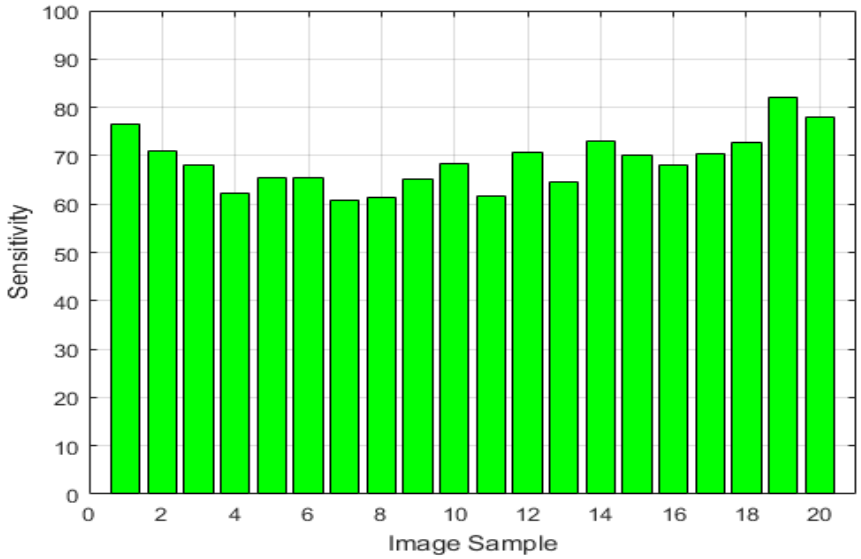

Figure 4.10 Sensitivity of each images from DRIVE database.

The specificity of each image from DRIVE database shows below in Figure 4.11

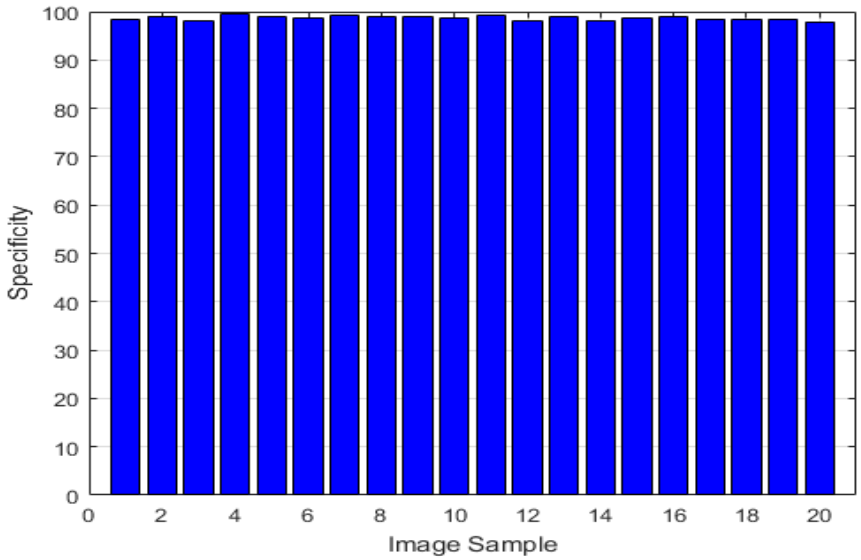

Figure 4.11 Specificity of each image from DRIVE database.

The Accuracy of each image from DRIVE database shows in Figure 4.12

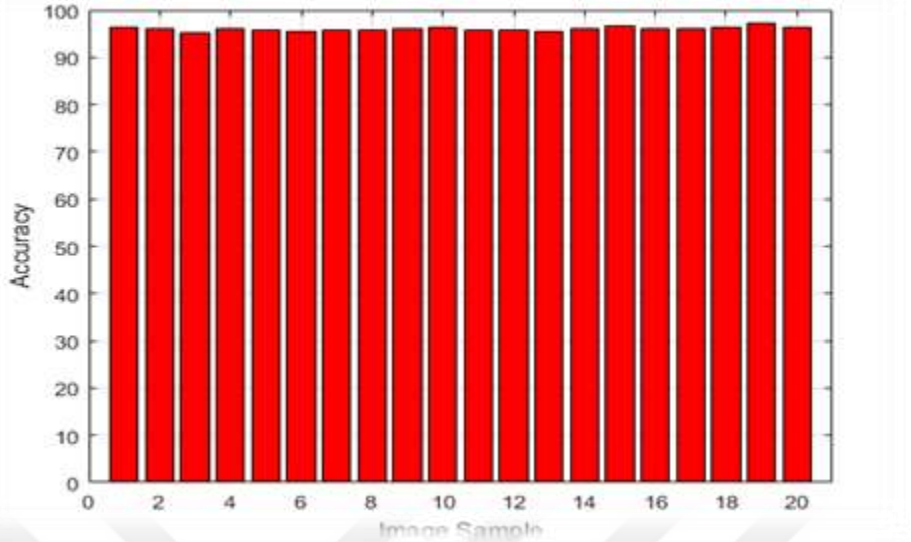

Figure 4.12 Accuracy of each image from DRIVE database.

In Figure 4.13, the results for two samples of the DRIVE database is shown.

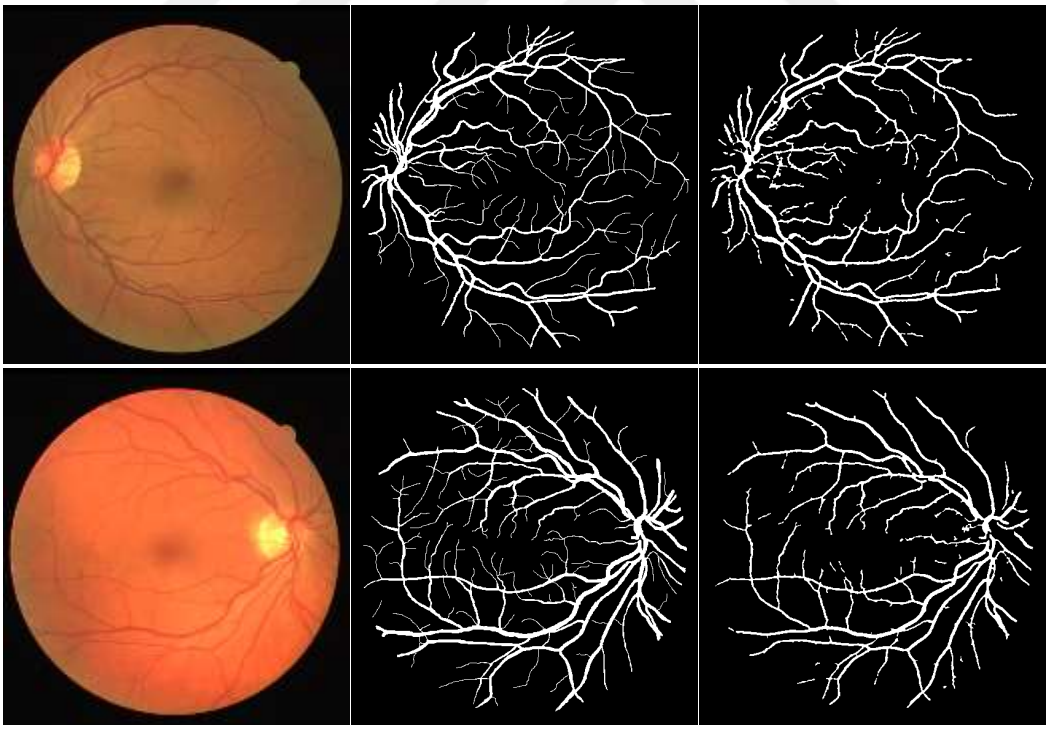

(a) (b) (c)

Figure 4.13 a) Original DRIVE image [41], **b)** Ground truth, **c)** Proposed result.

As shown in figure 4.13 the segmented blood vessel has a good result as comparing with the ground truth result.

4.2 Simulation Results for STARE Database

For STARE database, the result is shown in Table 4.2.

Table 4.2 Result of accuracy.

Image Number	Sensitivity	Specificity	Accuracy
1	0.732181	0.963595	0.945126
2	0.641411	0.970693	0.948763
3	0.820122	0.95062	**0.94281**
4	0.707565	0.967606	0.948328
5	0.709779	0.975055	0.951091
6	0.734811	0.98017	0.963081
7	0.838985	0.979597	0.968328
8	0.83239	0.976491	0.965733
9	0.821165	0.979805	0.967327
10	0.778695	0.966221	0.95114
11	0.803943	0.983975	0.971145
12	0.864523	0.983841	0.974614
13	0.778043	0.97929	0.961374
14	0.768874	0.98303	0.963632
15	0.736567	0.980493	0.959429
16	0.599981	0.986183	0.946749
17	0.763185	0.990705	0.970342
18	0.687553	0.992909	**0.977466**

19	0.765963	0.980583	0.971336
20	0.672411	0.968045	0.948316
Average	0.7529	0.9769	**0.9598**

As shown in Table 4.2 the average of all images are calculated, and the value of the proposed method is 0.9598 for accuracy. Also, the highest value for the accuracy is 0.977466. The lowest value for accuracy is obtained 0.94281 for image number 3.

The sensitivity of each image from STARE database shows below in Figure 4.14

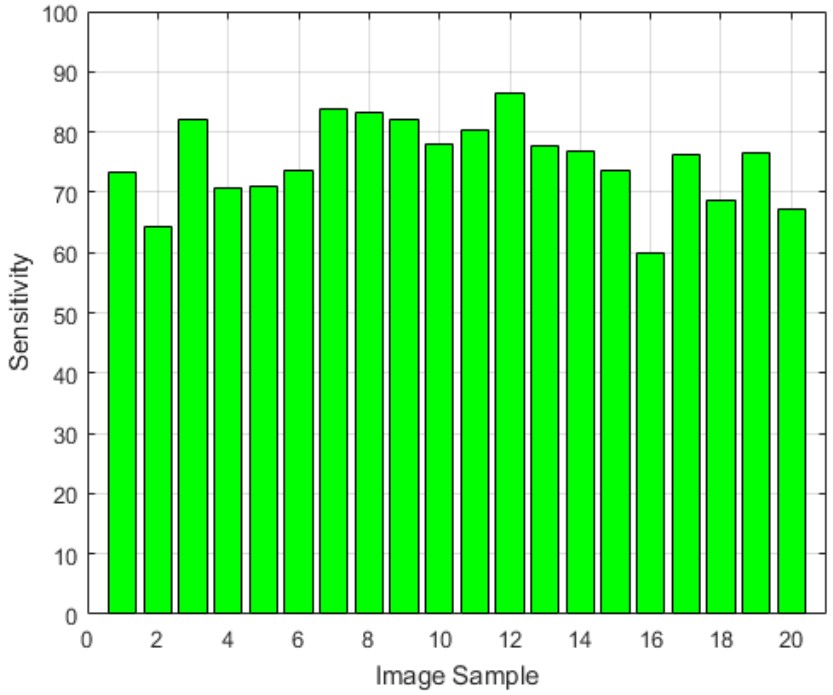

Figure 4.14 Sensitivity of each image from STARE database.

The specificity of each image from STARE database shows below in Figure 4.15

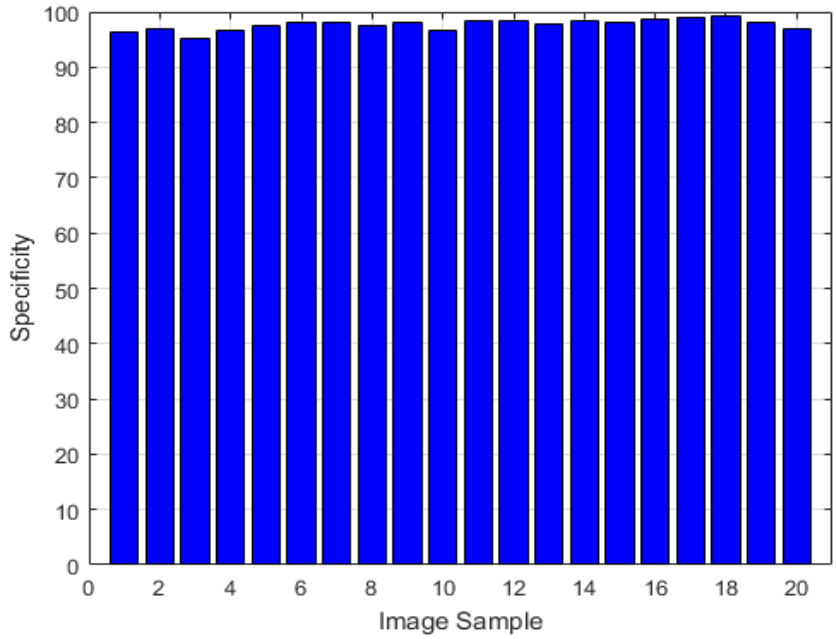

Figure 4.15 Specificity of each image from STARE database**.**

The accuracy of each image from STARE database shows below in Figure 4.16

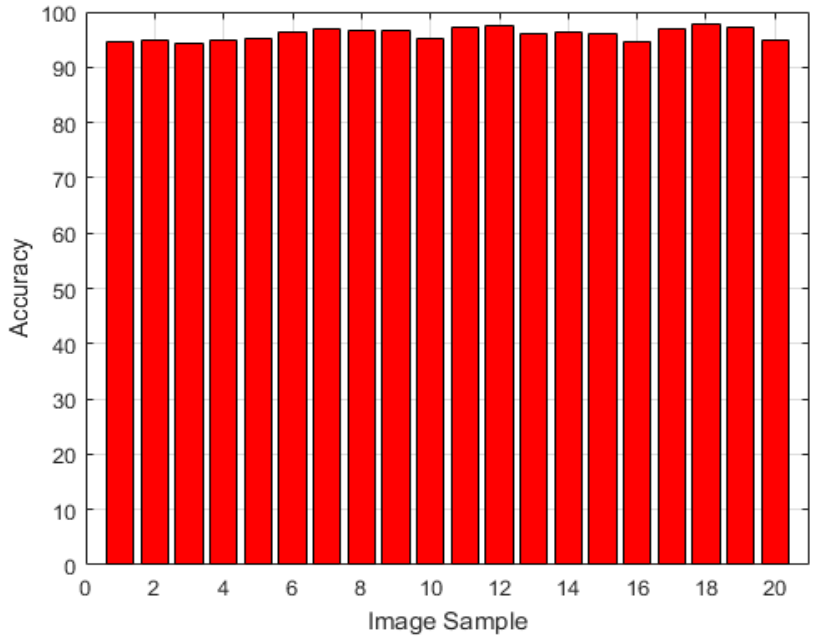

Figure 4.16 Accuracy of each image from STARE database.

In Figure 4.17 the result for two sample of the STARE database is shown.

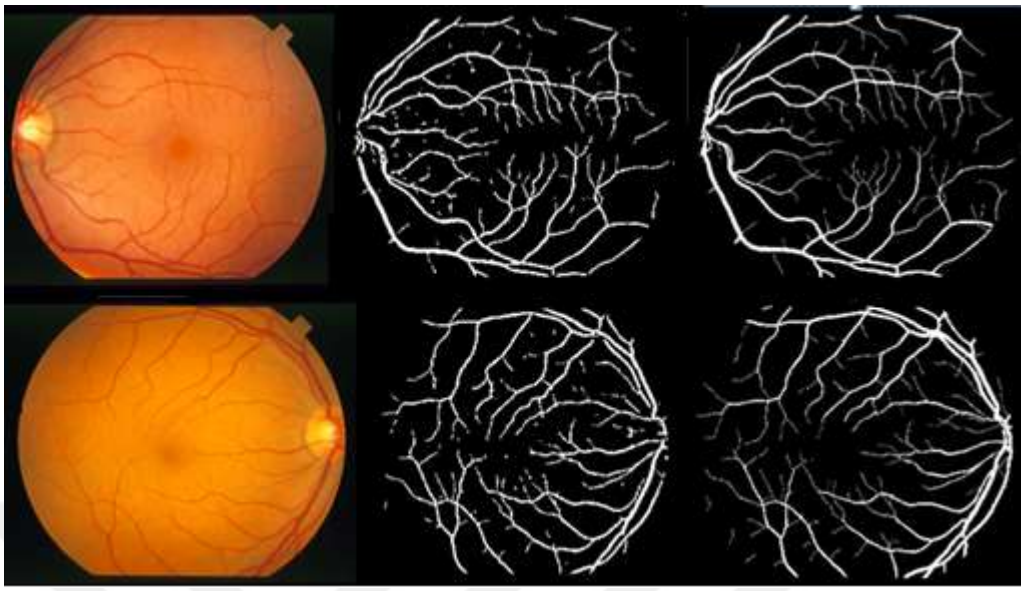

(a) (b) (c)

Figure 4.17 a) Original STARE image [2], **b)** Ground truth, **c)** Proposed result.

As a result, for STARE database, the segmented vessels have high performance result as comparing with the ground truth result.

The processing time for DRIVE and STARE database is illustrated in Table 4.3.

Table 4.3 The processing time for DRIVE and STARE database.

Database	**DRIVE**	**STARE**
1	0.428215	0.144925
2	0.439556	0.294599
3	0.373277	0.253
4	0.167547	0.209555
5	0.51407	0.297416
6	0.156387	0.172431
7	0.149385	0.180442

8	0.151064	0.183578
9	0.157059	0.181682
10	0.152955	0.176993
11	0.148658	0.185166
12	0.152584	0.177415
13	0.149948	0.174728
14	0.154561	0.178981
15	0.147963	0.185286
16	0.150159	0.186308
17	0.153462	0.188481
18	0.151695	0.18173
19	0.150924	0.182947
20	0.152753	0.185592
Average	**0.2101**	**0.1961**

The comparison between the processing time for DRIVE and STARE database for our method where STARE database was faster than DRIVE database but for accuracy was more accurate. The comparison between our method and other methods is shown in Table 4.4.

Table 4.4 A comparison of a new method and previous methods.

Name	Method	Accuracy DRIVE	Accuracy STARE
Zhang et al.in 2007 [26]	Nonlinear orthogonal projection	0.964	0.908
Marin et al.in 2011[25]	Gray-level and moment-invariant feature extraction methods	0.945	0.952
Fraz et al. 2011 [31]	Line strength and multiscale Gabor and morphological features	0.9470	0.95**7**
Oliveira et al. 2012 [28]	ORSF method	0.956	0.958
Asad.et al. in 2013 [29]	Water flooding model	0.937	
Nguyen et al.in 2013 [30]	Using multi-scale line detection	0.940	0.932
Fraz et al. in 2013 [27]	Linear discriminant classifier	0.950	**0.962**
Emray et al.in 2014 [32]	Bee colony optimization	0.939	0.947
Hassan et al.in 2015 [33]	Mathematical morphology and K-means clustering	0.951	

Hameed et al. In 2015 [34]	The pixel tracking algorithm filters	0.940	0.954
Imani et al.in 2015 [35]	MCA algorithm and Morlet wavelet transform	0.9523	0.9590
Mapayi et al.in 2015 [36]	(GLCM) matrix and fuzzy c - mean value	0.9473	0.9354
Mehta et al. in 2016 [37]	Morphological operations and The Rician Denoise method	0.9449	0.9435
Fan et al. in 2017 [38]	Region Features and Hierarchical Growth Algorithm	0.960	0.957
Our proposed method	**Morphological methods**	**0.961**	**0.959**

As shown in Table 4.4 the proposed method has high accuracy for DRIVE and STARE database than the other methods. For DRIVE database, the best performance is 0.961 and for STARE database is 0.959.

In this thesis, the graphical user interface (GUI) is used for good showing of the result. This GUI is shown in Figure 4.18.

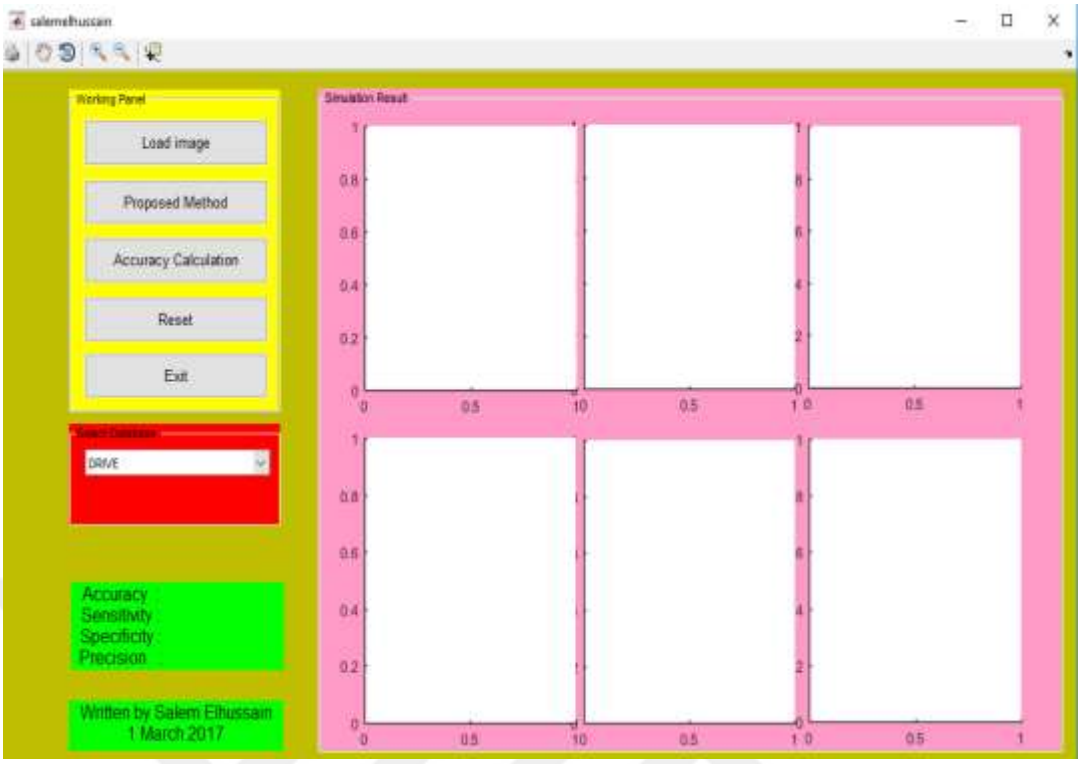

Figure 4.18 GUI for proposed method in the thesis.

With selecting the load image button, the image and ground truth and mask are loaded and shown in the GUI. This is shown in Figure 4.19. Also, there is the option for selecting the DRIVE database and STARE database.

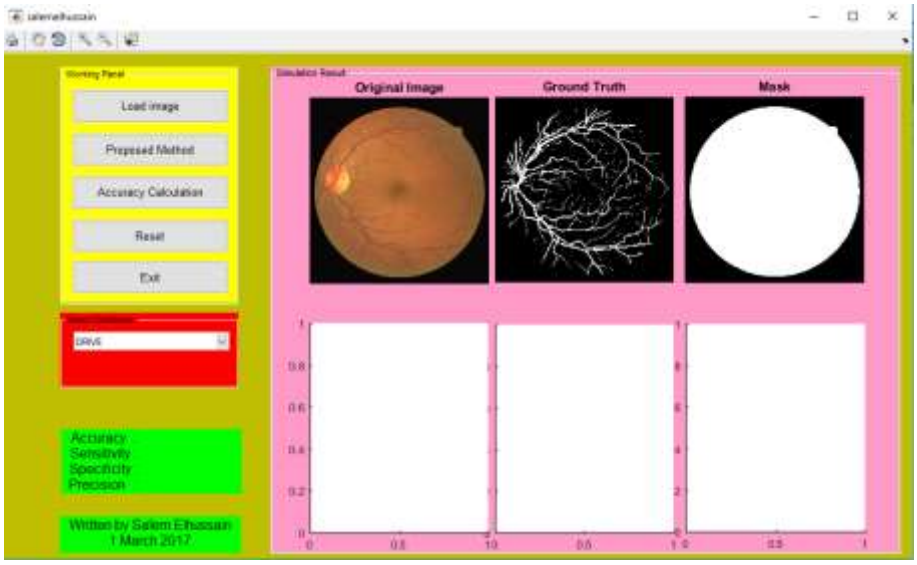

Figure 4.19 Result of the GUI when select the load image bottom.

After clicking on the proposed method bottom, the algorithm starts to find the vessel as mentioned in previous sections. This result is shown in Figure 4.20.

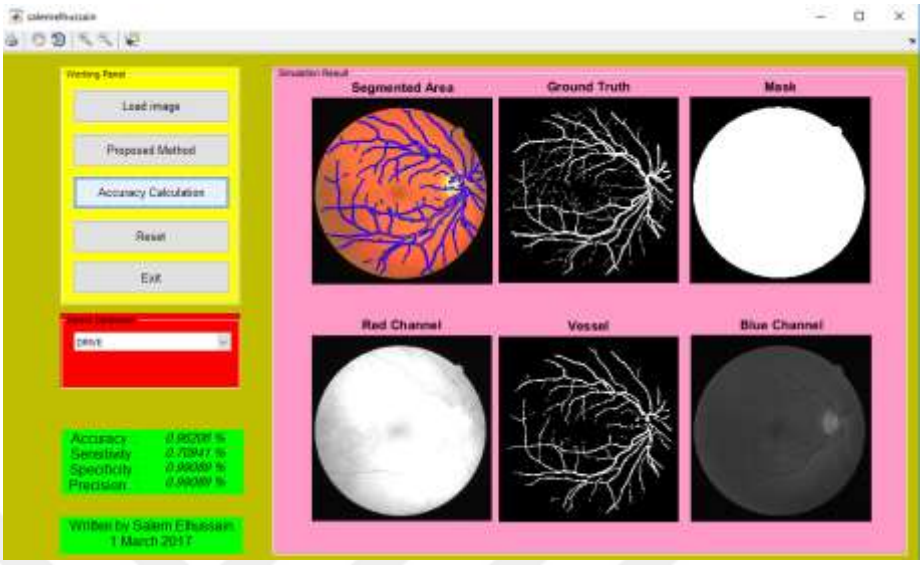

Figure 4.20 Result of the GUI after clicking on the proposed method.

As seen in Figure 4.20, the accuracy, sensitivity, specificity and precision are shown.

CHAPTER 5

CONCLUSIONS AND FUTURE WORKS

5.1 Conclusions

Retina blood vessel segmentation is one of the main important steps in the surgery of the eye. The imaging system is taken by the fundus camera. A fundus camera, also a retinal camera, is an ophthalmological device which is used to take photographs of the posterior sections of the eye (retina). The images support the diagnosis of ophthalmology and serve to make visible changes and to document these changes. In the conventional investigation of the ocular fundus using slit lamp microscopy or ophthalmoscopy, the middle retinal areas up to 50-60 ° had to be usually enlarged to obtain an unobstructed view. A fundus camera is equipped with a commercially available digital reflex camera as well as a ring flash which allows high-resolution images which can be stored in a digital patient's file or can be stored in the card format in printed form. As a result, unlike in the case of examinations by using a slit lamp or ophthalmoscope, a subsequent assessment by third parties or a control of the course of the disease is possible. In this thesis, the retinal vessel segmentation is investigated, and the new algorithm is introduced. The morphological methods are used for the filtering and extraction for the vessel. For contrast, methods of morphological building elements are used. For background cleaning, a 25x25 median filter is used and then the median filter is removed from the final image. This technique is the background. Also, the threshold method for binarization is used. This value gave us better results than the other values.

The advantage of proposed method is not complexity and have high accuracy than the other method which compared in this study. For thresholding of the vessel or Non-vessel areas, the Otsu method is used. The DRIVE and STARE database are used for implementation of the method. Sensitivity, specificity, and accuracy are used for evaluation of the proposed algorithm. The average of the accuracy for DRIVE database is 0.9606, and for the STARE database is 0.9598. For show the result as

graphically the Graphical User Interface (GUI) is used in MATLAB. With this tool the result can represented.

5.2 Future Work

In future works, there are some areas to improve algorithm performance. Only using the DRIVE and STARE image database evaluation algorithm may not be sufficient to fully analyze the algorithm. Thus, for the evaluation of the algorithm, other available image databases may be included to the study.

For the fast processing, the parallel processing algorithms can be added to the implementation. The MATLAB implementations cannot work so fast program but with using the parallel processing algorithms, it will be very fast and for the real-time applications, it will be a good solution.

REFERENCES

[1] H. Jelinek and M. J. Cree, *Automated image detection of retinal pathology*: CRC Press, 2009.

[2] X. Gao, A. Bharath, A. Stanton, A. Hughes, N. Chapman, and S. Thom, "A method of vessel tracking for vessel diameter measurement on retinal images," in *Image processing, 2001. Proceedings. 2001 International conference on*, pp. 881-884, 2001.

[3] H. R. Taylor and J. E. Keeffe, "World blindness: a 21st century perspective," *British Journal of Ophthalmology*, vol. 85, pp. 261-266, 2001.

[4] I. Liu and Y. Sun, "Recursive tracking of vascular networks in angiograms based on the detection-deletion scheme," *IEEE Transactions on Medical Imaging*, vol. 12, pp. 334-341, 1993.

[5] O. Chutatape, L. Zheng, and S. Krishnan, "Retinal blood vessel detection and tracking by matched Gaussian and Kalman filters," in *Engineering in Medicine and Biology Society, 1998. Proceedings of the 20th Annual International Conference of the IEEE*, pp. 3144-3149, 1998.

[6] E. Grisan and A. Ruggeri, "A divide et impera strategy for automatic classification of retinal vessels into arteries and veins," in *Engineering in medicine and biology society, 2003. Proceedings of the 25th annual international conference of the IEEE*, pp. 890-893, 2003.

[7] A. Hoover and M. Goldbaum, "Locating the optic nerve in a retinal image using the fuzzy convergence of the blood vessels," *IEEE transactions on medical imaging*, vol. 22, pp. 951-958, 2003.

[8] L. Gang, O. Chutatape, and S. M. Krishnan, "Detection and measurement of retinal vessels in fundus images using amplitude modified second-order Gaussian filter," *IEEE transactions on Biomedical Engineering*, vol. 49, pp. 168-172, 2002.

[9] S. Chaudhuri, S. Chatterjee, N. Katz, M. Nelson, and M. Goldbaum, "Detection of blood vessels in retinal images using two-dimensional matched filters," *IEEE Transactions on medical imaging*, vol. 8, pp. 263-269, 1989.

[10] B. Zhang, L. Zhang, L. Zhang, and F. Karray, "Retinal vessel extraction by matched filter with first-order derivative of Gaussian," *Computers in biology and medicine,* vol. 40, pp. 438-445, 2010.

[11] M. Al-Rawi, M. Qutaishat, and M. Arrar, "An improved matched filter for blood vessel detection of digital retinal images," *Computers in Biology and Medicine,* vol. 37, pp. 262-267, 2007.

[12] K. Sreejini and V. Govindan, "Improved multiscale matched filter for retina vessel segmentation using PSO algorithm," *Egyptian Informatics Journal,* vol. 16, pp. 253-260, 2015.

[13] M. E. Martinez-Perez, A. D. Hughes, S. A. Thom, A. A. Bharath, and K. H. Parker, "Segmentation of blood vessels from red-free and fluorescein retinal images," *Medical image analysis,* vol. 11, pp. 47-61, 2007.

[14] O. Hibet-Allah, J. Hajer, and H. Kamel, "Vascular tree segmentation in MRA images using Hessian-based multiscale filtering and local entropy thresholding," in *Advanced Technologies for Signal and Image Processing (ATSIP), 2016 2nd International Conference on*, pp. 325-329, 2016.

[15] L. C. Neto, G. L. Ramalho, J. F. R. Neto, R. M. Veras, and F. N. Medeiros, "An unsupervised coarse-to-fine algorithm for blood vessel segmentation in fundus images," *Expert Systems with Applications,* vol. 78, pp. 182-192, 2017.

[16] L. Wang, A. Bhalerao, and R. Wilson, "Analysis of retinal vasculature using a multiresolution hermite model," *IEEE Transactions on Medical Imaging,* vol. 26, pp. 137-152, 2007.

[17] H. Narasimha-Iyer, J. M. Beach, B. Khoobehi, and B. Roysam, "Automatic identification of retinal arteries and veins from dual-wavelength images using structural and functional features," *IEEE transactions on biomedical engineering,* vol. 54, pp. 1427-1435, 2007.

[18] B. Al-Diri, A. Hunter, and D. Steel, "An active contour model for segmenting and measuring retinal vessels," *IEEE Transactions on Medical imaging,* vol. 28, pp. 1488-1497, 2009.

[19] K. Sum and P. Y. Cheung, "Vessel extraction under non-uniform illumination: a level set approach," *IEEE Transactions on Biomedical Engineering,* vol. 55, pp. 358-360, 2008.

[20] L. C. Rodrigues and M. Marengoni, "Segmentation of optic disc and blood vessels in retinal images using wavelets, mathematical morphology and Hessian-based multi-scale filtering," *Biomedical Signal Processing and Control,* vol. 36, pp. 39-49, 2017.

[21] A. Osareh and B. Shadgar, "Automatic blood vessel segmentation in color images of retina," *Iranian Journal of Science and Technology,* vol. 33, p. 191, 2009.

[22] L. Xu and S. Luo, "A novel method for blood vessel detection from retinal images," *Biomedical engineering online,* vol. 9, p. 14, 2010.

[23] C. A. Lupascu, D. Tegolo, and E. Trucco, "FABC: retinal vessel segmentation using AdaBoost," *IEEE Transactions on Information Technology in Biomedicine,* vol. 14, pp. 1267-1274, 2010.

[24] X. You, Q. Peng, Y. Yuan, Y.-m. Cheung, and J. Lei, "Segmentation of retinal blood vessels using the radial projection and semi-supervised approach," *Pattern Recognition,* vol. 44, pp. 2314-2324, 2011.

[25] D. Marín, A. Aquino, M. E. Gegúndez-Arias, and J. M. Bravo, "A new supervised method for blood vessel segmentation in retinal images by using gray-level and moment invariants-based features," *IEEE Transactions on medical imaging,* vol. 30, pp. 146-158, 2011.

[26] Y. Zhang, W. Hsu, and M. L. Lee, "Segmentation of retinal vessels using nonlinear projections," in *Image Processing, 2007. ICIP 2007. IEEE International Conference on*, pp. V-541-V-544, 2007.

[27] M. M. Fraz, P. Remagnino, A. Hoppe, S. Velastin, B. Uyyanonvara, and S. Barman, "A supervised method for retinal blood vessel segmentation using line strength, multiscale Gabor and morphological features," in *Signal and Image Processing Applications (ICSIPA), 2011 IEEE International Conference on*, pp. 410-415, 2011.

[28] W. S. Oliveira, T. I. Ren, and G. D. Cavalcanti, "An unsupervised segmentation method for retinal vessel using combined filters," in *Tools with Artificial Intelligence (ICTAI), 2012 IEEE 24th International Conference on*, pp. 750-756, 2012.

[29] A. H. Asad, E. El Amry, and A. E. Hassanien, "Retinal vessels segmentation based on water flooding model," in *Computer Engineering Conference (ICENCO), 2013 9th International*, pp. 43-48, 2013.

[30] U. T. Nguyen, A. Bhuiyan, L. A. Park, and K. Ramamohanarao, "An effective retinal blood vessel segmentation method using multi-scale line detection," *Pattern recognition,* vol. 46, pp. 703-715, 2013.

[31] M. Fraz, P. Remagnino, A. Hoppe, and S. Barman, "Retinal image analysis aimed at extraction of vascular structure using linear discriminant classifier," in *Computer Medical Applications (ICCMA), 2013 International Conference on*, pp. 1-6, 2013.

[32] E. Emary, H. M. Zawbaa, A. E. Hassanien, G. Schaefer, and A. T. Azar, "Retinal blood vessel segmentation using bee colony optimisation and pattern search," in *Neural Networks (IJCNN), 2014 International Joint Conference on*, pp. 1001-1006, 2014.

[33] G. Hassan, N. El-Bendary, A. E. Hassanien, A. Fahmy, and V. Snasel, "Retinal blood vessel segmentation approach based on mathematical morphology," *Procedia Computer Science,* vol. 65, pp. 612-622, 2015.

[34] I. Hameed, H. Ocbagabir, B. D. Barkana, and B. Yildirim, "Blood Vessel Segmentation in Retinal Images by Morphological Operations and by a Novel Pixel Tracking Algorithm," *International Journal of Innovative Computing, Information & Control: IJICIC,* vol. 11, pp. 189-202, 2015.

[35] E. Imani, M. Javidi, and H.-R. Pourreza, "Improvement of retinal blood vessel detection using morphological component analysis," *Computer methods and programs in biomedicine,* vol. 118, pp. 263-279, 2015.

[36] T. Mapayi, J.-R. Tapamo, and S. Viriri, "Retinal vessel segmentation: a comparative study of fuzzy C-means and sum entropy information on phase congruency," *International Journal of Advanced Robotic Systems,* vol. 12, p. 133, 2015.

[37] K. Mehta and N. Kaur, "An Enhanced Segmentation Technique for Blood Vessel in Retinal Images." International Journal of Computer Applications, Vol 150,pp.0975 – 8887, 2016.

[38] Z. Fan, J. Lu, and W. Li, "Automated Blood Vessel Segmentation of Fundus Images Based on Region Features and Hierarchical Growth Algorithm," *arXiv preprint arXiv:1701.00892*, 2017.

[39] Y. Zhang, W. Hsu, and M. L. Lee, "Detection of retinal blood vessels based on nonlinear projections," *Journal of Signal Processing Systems*, vol. 55, pp. 103-112, 2009.

[40] B. Ristic, S. Arulampalam, and N. Gordon, *Beyond the Kalman filter: Particle filters for tracking applications* vol. 685: Artech house Boston, 2004.

[41] J. Staal, M. D. Abràmoff, M. Niemeijer, M. A. Viergever, and B. Van Ginneken, "Ridge-based vessel segmentation in color images of the retina," *IEEE transactions on medical imaging*, vol. 23, pp. 501-509, 2004.

[42] T. Chanwimaluang, G. Fan, and S. R. Fransen, "Hybrid retinal image registration," *IEEE transactions on information technology in biomedicine*, vol. 10, pp. 129-142, 2006.

[43] R. C. Gonzales and P. Wintz, "Digital image processing ", 1987.

[44] D. H. Parks and S. S. Fels, "Evaluation of background subtraction algorithms with post-processing," in *Advanced Video and Signal Based Surveillance, 2008. AVSS'08. IEEE Fifth International Conference on*, pp. 192-199, 2008.

[45] http://docs.opencv.org/trunk/d1/dc5/tutorial_background_subtraction.html.

[46] N. Senthilkumaran and S. Vaithegi, "Image segmentation by using thresholding techniques for medical images," *Computer Science & Engineering: An International Journal*, vol. 6, 2016.

[47] R. Gonzalez and P. Wintz, "Digital image processing" , 1977.

[48] M. Niemeijer, J. Staal, B. van Ginneken, M. Loog, and M. D. Abramoff, "Comparative study of retinal vessel segmentation methods on a new publicly available database," in *SPIE medical imaging*, pp. 648-656, 2004.

CIRRICULUM VITAE

PERSONAL INFORMATION

Name Surname: SALEM.ELHUSSAIN

Date of Birth: 16/05/1985

Phone: 5439125518

E-mail : Elhussain.salem@yahoo.com

EDUCATION

Bachelor: University of Omar Mukhtar Darna – Libya (2004 -2008)

Master Degree: Ankara Yıldırım Beyazıt University (2015-continued)

PROFESSIONAL EXPERIENCE

Research Assist: Omar Mukhtar University (2009- continued)

TOPICS OF INTERESTS

- Image Processing - Digital Signal Processing

- Signal Processing

HOBBIES

Traveling and Reading